MATERIALS PHYSICS AND MECHANICS RESEARCH ARTICLE

Submitted: January 23, 2026 **Revised: February 7, 2026** **Accepted: July 2, 2026**

Prediction of properties of high-performance concrete containing glass fibers and minibar basalt using AI-based criteria

N.I. Vatin [1], M. Hematibahar [2]✉, T.H. Gebre [2,3]

[1] Peter the Great St. Petersburg Polytechnic University, Saint Petersburg, Russia

[2] RUDN University, Moscow, Russia

[3] Moscow State University of Civil Engineering (National Research University), Moscow, Russia

✉ eng.m.hematibahar1994@gmail.com

ABSTRACT

The aim of the study is to predict compressive strength and the failure mechanism of concrete cubes considering the Tresca criterion for high-performance concrete reinforced with glass fibers and minibar basalt. The method of research includes experimental compression tests on 100 mm cubes at curing ages of 7, 14 and 28 days soft computing techniques such as linear regression ridge regression and polynomial regression implemented in Python using scikit-learn artificial neural networks developed with Python and NumPy to visualize cracks and failure patterns as pixels as well as the incorporation of the Mohr-Coulomb and Tresca criteria to model the plastic zone and pyramidal failure shape. The results demonstrate that polynomial regression provides the highest predictive accuracy for compressive strength achieving R2 values greater than 0.99 for minibar basalt fiber-reinforced high-performance concrete and greater than 0.93 for glass fiber-reinforced high-performance concrete while the artificial neural networks successfully identify and predict crack locations failure degree and pyramidal failure shapes and overall model performance is validated by a coefficient of determination greater than 0.97 with mean absolute error greater than 2.1 and root mean square error greater than 16.99 confirming strong agreement between experimental and predicted values. Therefore, the research's novelty lies in its use of artificial intelligence by taking into account the TRESCA criteria to precisely predict the properties of high-performance concrete and to understand the impact of its input factors, streamlining the process and providing useful tools for the real-world application of the model's capabilities in the field of civil engineering.

KEYWORDS

deformation and fracture processes • strength and plasticity • Tresca criterion • fiber-reinforced concrete failure mechanisms • glass fibers and minibar basalt

Funding. *This research was funded by the Ministry of Science and Higher Education of the Russian Federation within the framework of the state assignment No 075-03-2025-256 dated 16 January 2025, Additional agreement No 075-03-2025-256/1 dated 25 March 2025, FSEG-2025-0008.*

Citation: Vatin NI, Hematibahar MH, Gebre TH. Prediction of properties of high-performance concrete containing glass fibers and minibar basalt using AI-based criteria. *Materials Physics and Mechanics*. 2026;54(4): 173–192.
http://dx.doi.org/10.18149/MPM.5442026_14

Introduction

High-performance concrete is a high-tech concrete with special admixtures that improve mechanical properties, workability, and internal consistency. The extend ed lifespan, along with HPC's security features, makes it an appealing option for building projects. Despite the well-known remarkable compressive strength of regular concrete, its fundamental tension weakness has significant drawbacks. To solve these drawbacks, basalt fiber (BF) is used as

© N.I. Vatin, M.H. Hematibahar, T.H. Gebre, 2026.
Publisher: Peter the Great St. Petersburg Polytechnic University
This is an open access article under the CC BY-NC 4.0 license (https://creativecommons.org/li-censes/by-nc/4.0/)

a reinforcing material [1]. It is also used as a building material due to its distinct mechanical properties and robust resistance to heat, alkali, and rust. Basalt fiber (BF) is a high-strength mechanical fiber [2]. As a result, BF is less expensive than other fibers because it requires only one processing step. Basalt fiber is used for a variety of purposes, including wiring, sports equipment, automotive parts, and fire prevention. Studies indicate growing interest in applying BF to other sectors, reflecting broader use for various objectives. Because BF improves mechanical, chemical, and thermal stability, it has become increasingly used as a building material [3–5]. Another justification for incorporating basalt fibers into high-performance concrete is to improve its tensile, bending, and long-term performance [6,7]. The study found that basalt fiber-infused high-strength concrete outlasted regular high-strength concrete in terms of durability. The notably higher bending and tensile strengths of HPC illustrate the advantages of incorporating basalt fibers [8–10]. Basalt fibers have cost benefits in addition to their desirable mechanical qualities [11]. Adding 0.4 to 1.8 % of basalt fiber to high-performance concrete alters its mechanical properties. Meanwhile, 1.2 % of BF samples had high flexural strength [12,13]. Some studies investigated the addition of silica fume and BF to high-performance concrete. Adding silica fume to high-performance concrete reduces the mix's porosity [14]. The consolidation of high-performance concrete increases its strength. Similarly, several percentages of basalt fiber in high-performance concrete were examined and analyzed [15]. Another study showed that adding 1.33 % BF to high-performance concrete results in the flexural and tensile strengths reaching their maximum [16]. The tensile and compressive strengths of concrete were found to be positively influenced by fiber element lengths and sizes relatively than self-weight of fiber proportions with in the mix.

To perform the study, a compression test has been undergone by a considering standard cubic samples in compliance with the requirements set forth by the American Society for Testing and Materials and the Russian Standard Code Design [17,18]. The conventional procedure, commonly referred to as the standard destructive test, is frequently used for testing concrete's mechanical properties. In the testing facility, various samples has to be taken to evaluate the concrete's compressive strength [19]. The standard destruction method may not provide accurate results for a variety of reasons, including the interfacial transition zone, the water-to-cement ratio, the fine aggregate modulus, the kind and size of the cement and aggregate, and so on. Taking all of these factors into consideration, various methods for predicting the mechanical properties of concrete were developed, including the use of nondestructive technologies to validate the results against established criteria [20]. As a result, a reliable prediction model for the mechanical properties of high-performance concrete structures based on artificial intelligence is necessary to broaden its application in construction while maintaining its performance.

Destructive testing on existing concrete structural members is costly and risky due to the properties of the material [21]. If destructive testing using core samples is not feasible, nondestructive testing (NDT) can be used as an alternative or in conjunction with destructive testing techniques to assess concrete strength in existing structures quickly [22,23]. As a result, a reliable prediction model for mechanical properties of high-performance concrete structures based on artificial intelligence is necessary to broaden its application in construction while maintaining its performance.

Recent developments in artificial intelligence have made machine learning techniques a fascinating modeling tool that may be used to many scientific fields, such as material and structural engineering. Therefore, it is currently popular to predict concrete characteristics using artificial intelligence by taking into account TRESCA criterion techniques. These programs can be used for a variety of tasks, including linear regression, ridge regression, polynomial regression etc. [23–34]. Concrete compressive strength relies on statistical relationships between nondestructive factors and test parameters, necessitating extra processes for nondestructive variables utilized in classical regression analysis [35–37]. The equations and algorithms may be converted from classical programming to computer programs using predictive techniques, which are an alternative and efficient way that can save time and money [16]. An algorithmic programming method was developed as part of nondestructive methods to forecast concrete compressive strength at various curing ages [38]. In general, the research indicates that the laboratory test results closely match the expected compressive strength of the developed method across all conventional concrete curing timeframes. As a mechanical property prediction technique that accounts for mixed design attributes, artificial neural networks (ANNs) may also be used [39,40]. The results of the investigation demonstrated the validity of the ANNs' predictions by demonstrating how closely the outcomes correspond with the results of the experiment. The original concrete mixture's concrete strength was investigated using the multiple linear regression (MLR) method [40–42]. The study's findings proved that the MLR estimation method for the first concrete was effective.

Different types of data mining and machine learning, such as the strength of concrete and the shape and dimension of aggregates, are applied [31,43]. The size and shape of aggregates can be considered hyperparameters in Artificial neural network programming. Artificial neural networks and Fuzzy Logic (FL) techniques were examined independently for forecasting the composition of concrete with increased fly ash [32,44]. To predict concrete compressive strength, the investigator focused on aggregate diameter as a hyperparameter. Considering their results, the R^2 value is 0.9 [31,43]. For example, another researcher found that the R^2 value of 0.98 for Gaussian process regression GPR prediction accuracy. However, they studied Machine learning techniques, such as ensemble learning (EL), support vector machine regression (SVMR), and Gaussian process regression (GPR) [16,33–38,45–48].

According to studies that used machine learning to predict concrete mechanical properties, Polynomial Regression (PR) can accurately predict mechanical properties ($R^2 > 0.99$). To forecast the mechanical characteristics of cement, this study used soft computing, machine learning, and artificial neural networks (ANNs). High-Performance Concrete (HPC) reinforced with minibar basalt fibers and glass fibers was the subject of the study. The mechanical behavior of HPC was modeled using a logistic function. Additionally, the compressive strength of HPC with minibar basalt and glass fibers was estimated using linear, ridge, and polynomial regression. By analyzing pixel data and mathematical formulae, artificial neural networks (ANNs) were used to investigate the failure mechanism of concrete cubes in addition to strength prediction. The ANN effectively replicated fracture patterns using Python. In order to validate the results, performance measures including the correlation coefficient (R^2), mean absolute error (MAE), and root mean square error (RMSE) were used to evaluate the prediction models' accuracy.

Materials and Methods

Experimental findings on fiber-reinforced high-performance concrete

To find the optimal performance of basalt fiber-reinforced high-performance concrete (BFC), concentrating primarily on maximizing the ratios of minibar basalt fibers (MBF) and supplemental glass fibers (GF), the current points have been studied:

1. HPC's remarkable mechanical qualities were preserved if basalt fibers were added, significantly increasing its tensile strength, flexural capacity, and durability.
2. The dependability of compressive concrete for a concrete cube sample has been examined as per the universal material testing standards.

The curing periods in this study were 7, 14, and 28 days. The following stages were taken in the mixing and preparation process:

1. Mixing procedure: in accordance with the designated concrete mix design, a 133-liter SB small mixer was used to combine the two aggregate types for two minutes. Concrete chemical powder was added after water, and cement and aggregates were mixed for more than 2 min. The mixer operated at a steady 48 rpm (Fig. 1(a)).
2. Concrete cubes are molded into 100 mm cubes. To start the hydration process, freshly cast samples were submerged in water at 20 °C for 48 h.
3. Moist vuring: Specimens were moved to a wet-curing chamber maintained at 15 °C for 7, 14, or 28 days after demolding (Fig. 1(c)).
4. Preparing for testing: cube surfaces were cleaned and dried to remove any imperfections before the compression testing (Fig. 1(d)). The removal ensured reliable, consistent measurements of compressive strength.

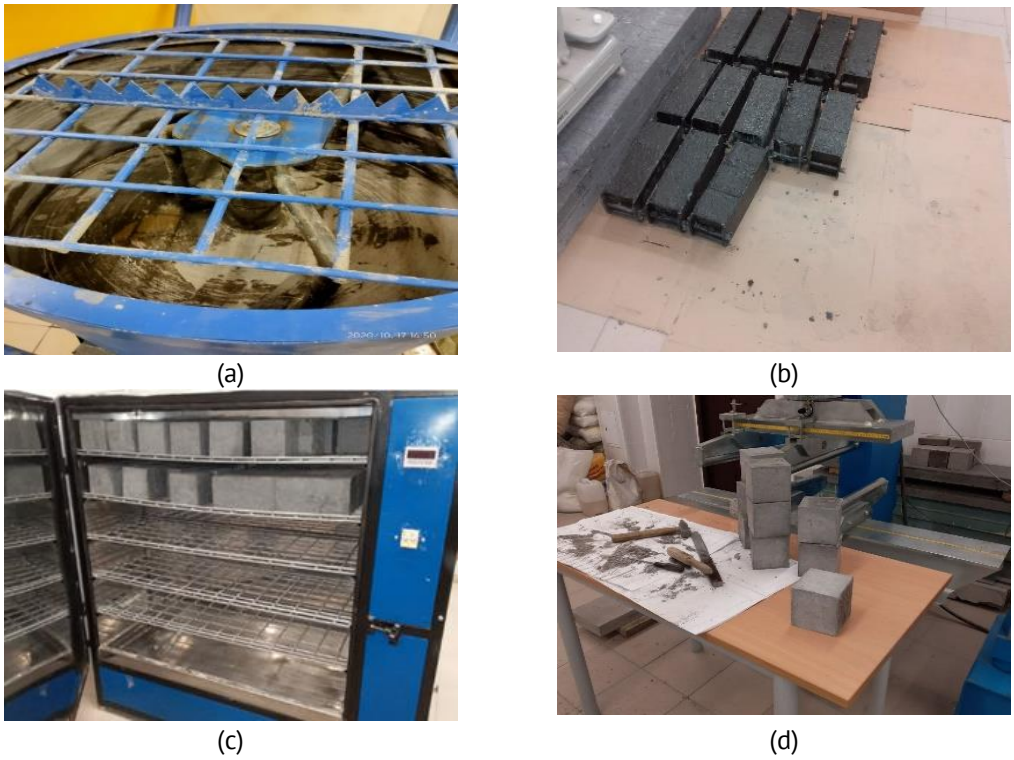


Fig. 1. Mixing and molding apparatuses, procedure, and cube specimens: (a) pan mixer; (b) concrete formwork; (c) moist cabinet; (d) samples cleaning process

With a maximum load capacity of 1300 kN, a C025N compression testing machine was used to assess the materials' compressive strength and stress-strain behavior. Precise measurements of failure loads and deformation properties under axial loading were possible with this testing machine. The following materials were used to make BFC: ordinary Portland cement (OPC), tap water, quartz flour, microsilica, crushed granite, quartz sand, superplasticizer, tap water, glass fiber, and basalt fiber (minibar). Table 1 displays the configurations of glass and basalt fibers used in this experiment based on their specific characteristics.

Table 1. Basalt fibre and glass fiber characteristics

Type	Cut length, mm	Diameter, mm	Tensile strength, MPa	Elastic modulus, GPa
Basalt Fibre	18	1.2	1080	44
Glass fiber	18	1.2	3420	72.4

Crushed granite was used as aggregate to increase compressive strength; micro silica was added to fill voids between the cementitious and BF. In practical applications, the BF can improve the mechanical properties of high-performance concrete, particularly its tensile and flexural strengths. Table 2 shows the basalt fiber percentages and mixture percentages for high-performance concrete. Six types of concrete samples with different percentages of basalt fiber (0, 0.6, 0.8, 1.2, 1.5, and 1.8) have been added to high-performance concrete. Meanwhile, the cement-to-water ratio was 0.375, the cement-to-aggregate ratio was 0.315, the plasticizer was 12.5 kg/m^3, the quartz flour was 100 kg/m^3, and the micro silica was 125 kg/m^3.

Table 2. The compositions, mixture design and percentages of basalt fiber concrete

Mix Code	BFC	BFC-6	BFC-9	BFC-1.2	BFC-1.2	BFC-1.8
Water-cement ratio	0.375	0.375	0.375	0.375	0.375	0.375
Cement per aggregates (sand + gravel) ratio	0.315	0.315	0.315	0.315	0.315	0.315
Micro silica, kg/m^3	125	125	125	125	125	125
Plasticizing, kg/m^3	12.5	12.5	12.5	12.5	12.5	12.5
Quartz flour, kg/m^3	100	100	100	100	100	100
Fiber dosage, %	-	0.6	0.9	1.2	1.5	1.8

In the present study, 1.2 % basalt fiber added to concrete could yield the mix's maximum mechanical strength. The compressive strength of glass and basalt fiber-equipped high-performance concrete minibars can be observed in Table 3 and Fig. 2.

Table 3. The static compressive strength of glass and mainbars basalt fiber high-performance concrete

Mix code	Compressive strength, MPa	
	Glass fiber high-performance concrete	Minbars basalt fiber high-performance concrete
BFC	101.43	101.43
BFC-06	92.78	101.4
BFC-09	92.68	105
BFC-1.2	102.3	90.5
BFC-1.5	97.06	89.5
BFC-1.8	95.68	92.3

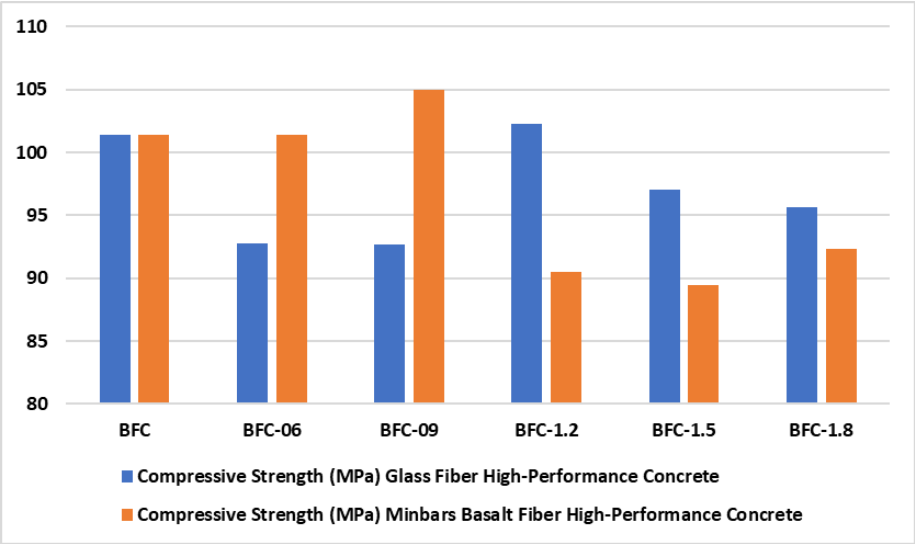


Fig. 2. Compressive strength of glass and mainbars basalt fiber high-performance concrete

High-performance concrete

A lower binding agent-to-water ratio and a higher fine aggregate volume can improve concrete's mechanical properties. Furthermore, microsilica can enhance the mechanical properties and durability of concrete. Adding fibers to concrete reduces the workability of both the concrete and the cement. In addition, fiber length and amount are related to concrete workability [49,50]. Numerous findings about the impact of basalt fibers have been made in the extent to which cementitious composites in compressive strength. As per other research, cementitious composites that contain basalt fibers exhibit a decrease in compressive strength at all dosages when compared to the control sample [51]. According to the current study, the best proportions for glass and minibar basalt fibers are considered as 1.2 and 0.9 %, respectively, and these values provide us the maximum compressive strength of the concrete mix [52,53].

Mohr-Coulomb and Tresca criteria

Using the Mohr-Coulomb (M-C) fracture criteria, the ductile fracture of materials without isotropic fissures is examined. This criterion has been widely applied in rock and soil mechanics because it accurately accounts for both the Lode angle parameter and the effects of hydrostatic pressure. The ability to forecast the fracture surface orientation uniquely is another benefit of the M-C fracture model. In the M-C criteria, it is demonstrated that the direction of the cosine of the unit normal vector to the fracture surface depends on the friction coefficient. It is quite possible to apply the phenomenological and physical M-C sound criteria as an engineering tool to anticipate ductile fracture using the Mohr-Coulomb equation [54,55].

$$\sigma_1(1 - sin\,\varphi) - \sigma_3(1 + sin\,\varphi) = 2c\,cos\,\varphi. \quad (1)$$

The Tresca and Mohr-Coulomb criteria use different methods, even though they are used to predict material failure. The Tresca criterion emphasizes a material's ultimate shear stress, whereas the Mohr-Coulomb criterion accounts for both normal and shear stresses in assessing failure. The Tresca yield criterion does not describe the effect of

hydrostatic pressure on an item. This criterion is applicable to concrete only as a simplification. This study considers Eq. (2), which defines the Tresca criterion:

$$\sigma_y = \frac{1}{2}(\sigma_1 - \sigma_3), \quad (2)$$

In principal-stress space the four classical yield criteria differ by the shape of the surface and by whether failure depends on hydrostatic pressure. The Tresca and von Mises criteria are independent of the mean stress: their surfaces are prisms (cylinders) aligned with the hydrostatic axis $\sigma_1 = \sigma_2 = \sigma_3$. In the deviatoric π -plane Tresca is a regular hexagon, whereas von Mises is the circle that circumscribes or is inscribed in that hexagon. The Mohr–Coulomb and Drucker–Prager criteria are pressure-sensitive: their surfaces are cones that open along the hydrostatic axis, so the admissible shear stress increases with confinement. In the π -plane Mohr–Coulomb is an irregular hexagon, which produces the well-known tension–compression asymmetry of concrete; Drucker–Prager is a circle and is therefore a smooth conical approximation to Mohr–Coulomb. Figure 3 compares the Tresca prism and the Mohr–Coulomb cone in this representation. Here θ is the Lode (deviatoric polar) angle, which locates the stress state on the hexagonal section, and φ is the internal friction angle, which controls the opening of the Mohr–Coulomb cone and vanishes for Tresca.

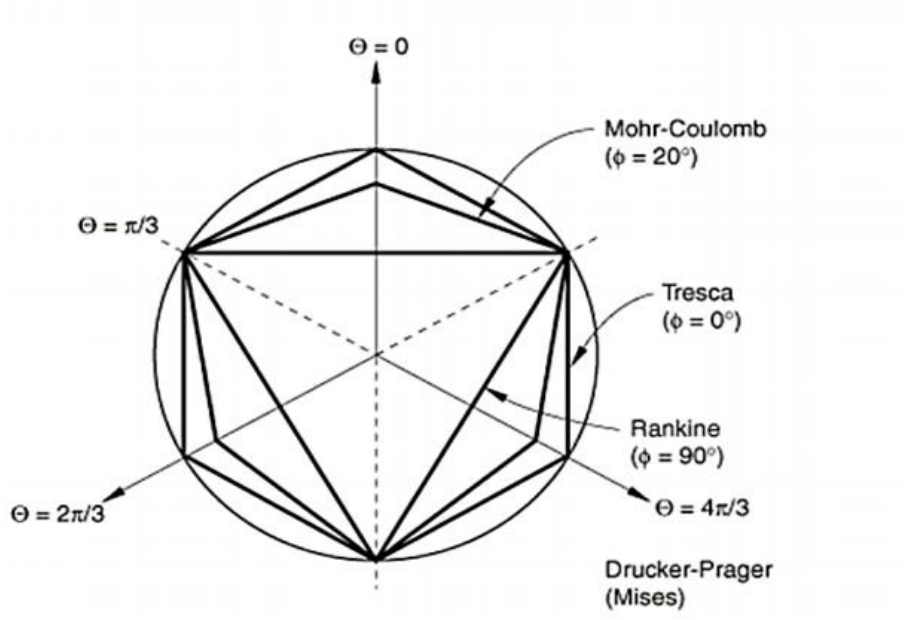


Fig. 3. Yield surfaces in principle-stress space and in the deviatoric (π) plane: the Tresca criterion (regular hexagon; prism along the hydrostatic axis) and the Mohr–Coulomb criterion (irregular hexagon; hexagonal cone). The von Mises and Drucker–Prager surfaces would appear as a circle in this plane (a circular cylinder and a circular cone, respectively)

In Fig. 3, θ is the deviatoric polar angle, and φ is the friction angle of the material. The compressive strength of concrete σ_m can be explained with the expression of equation (3), and it is based on [52]: By simulating a self-limiting stress feedback loop that determines failure thresholds on the multi-axial Tresca-Mohr-Coulomb surface, the non-linear constitutive coupling unifies pressure-sensitive yield criteria as shown below.

$$\sigma_m = \mu\sigma_m(\sigma_t - \sigma_m), \quad (3)$$

where μ is the friction or coupling Coefficient, σ_t is a total value, σ_m is the mean stress or microstructural stress.

According to the ACI 318-19[1], the concrete strain is equal to 0.003 of the compressive strength of concrete based on [37], and it is expressed in Eq. (4):

$$\sigma_m = \mu \cdot 9 \cdot 10^{-6}(f'_c), \quad (4)$$

$$\mu = \frac{f'_c}{\delta^2}, \quad (5)$$

where f'_c is the specified compressive strength of concrete, δ is the characteristic stress. Finally, the limitation equals the value in Eq. (4), as shown in Fig. 4.

Failure method

Concrete cubes tend to transfer compressive loading (σ_m) to tensile loading (σ_t) at the moment of failure. While reinforced fibers, such as basalt fibers, are resistant to tensile loading. At this moment, the plastic zone has been created due to the bridging effect of basalt fibers, as shown in Fig. 4.

After compression loading, the cube shape transforms into a pyramidal shape. At this moment, the crack ratio is known as φ, and the crack depth is d'; moreover, the length of the crack is L. Figure 5 shows the cracks happening in the cube under compression loads. According to Fig. 6, each element has deformation in the x and y directions, as expressed by Eq. (6):

$$d' = \left(\frac{\partial u_x}{\partial u_y} dy_n\right) + \left(\frac{\partial u_{n-1}}{\partial u_{n-1}} dy_{n-1}\right) + \cdots + \left(\frac{\partial u_1}{\partial u_1} dy_1\right), \quad (6)$$

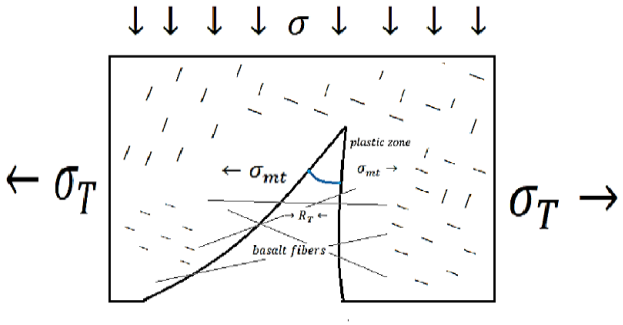


Fig. 4. The bridge effect on the cube compression

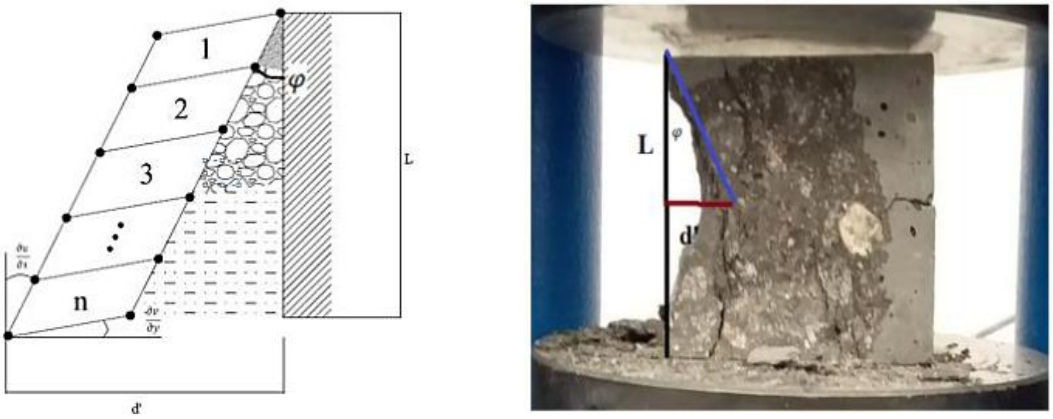


Fig. 5. The deformation of the failed concrete cross-section:
(a) deformation path elements (b) deformed concrete cubes

[1] American Concrete Institute. ACI 318-19. *Building Code Requirements for Structural Concrete (Inch-Pound Units)*. ACI; 2019.

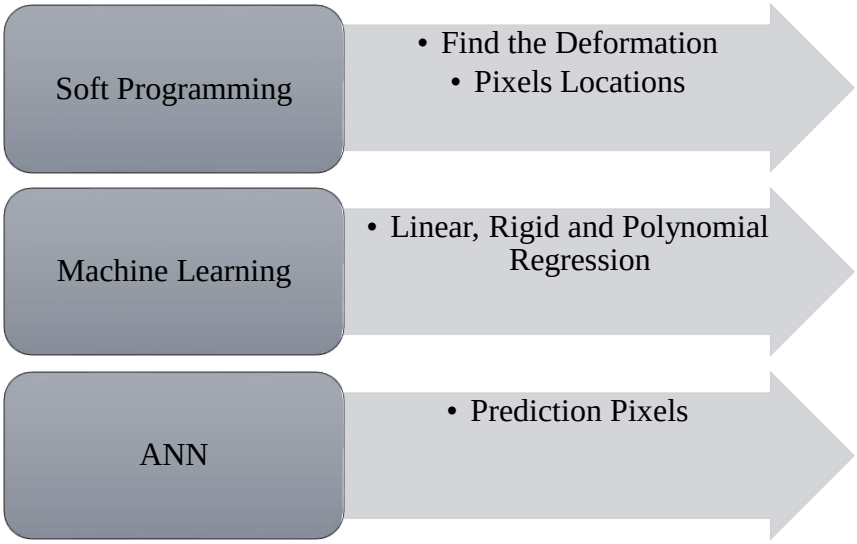
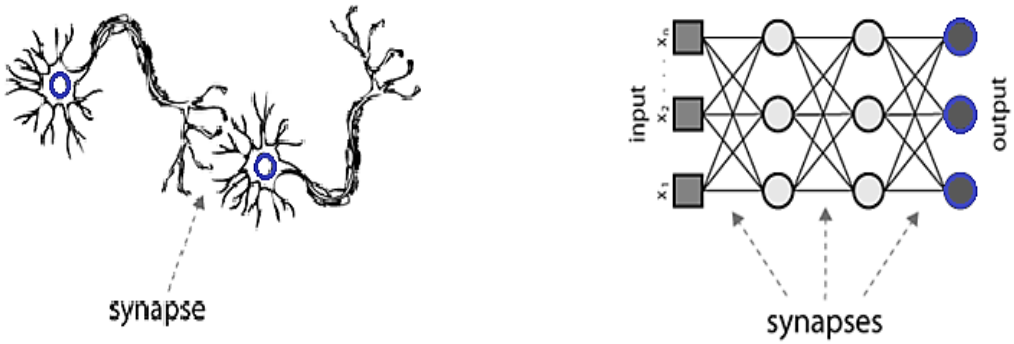


Fig. 6. The algorithm of the current study

Algorithm of study

The experimental findings of high-performance concrete reinforced with basalt fiber served as the foundation for the current investigation [56]. Predicted yield behavior, failure mechanisms, and validation of the Tresca criterion are expected outcomes, based on the experimental BFHPC test results (uniaxial/triaxial compression, flexural testing). Based on earlier research and experimental investigations on the HPC, Eq. (4) was discovered [33]. Equation (4), also referred to as the boundary in the M-C and Tresca criteria, can predict compressive strength. The M-C and Tresca criteria were used in the current investigation to predict concrete compressive strength. Taking into account the experimental BFHPC test data (flexural, uniaxial/triaxial compression), as well as the AI-predicted failure mechanisms, yield behavior, and validation of the Tresca criterion.

To validate the results, several evaluation indices were used, including the correlation coefficient (*R*), mean square error (*MSE*), root mean square error (*RMSE*), and mean absolute error [20]. As illustrated in Fig. 6, the current study's algorithm examines basalt fiber-reinforced high-performance concrete (BFHPC) using software programming, machine learning (ML) modeling, and artificial neural networks. It does this by predicting yield behavior, analyzing failures, and validating the Tresca criteria.



(a) (b)

Fig. 7. The artificial neural network: (a) biological neural network; (b) artificial neural network

The compressive strength of unified concrete (BFC) was predicted using linear, stiff, and polynomial regression models. These regressions were implemented using a machine learning model in Python's "skylearn" package. Additionally, the current study looked at concrete failure. Python was used to create simulation code to run the equation-based results. The deformation of each crack and failure piece has been established using prediction pixels. Next, the ANNs were established to find the pixels. Equation (6) is considered soft programming, and an ANN can help plot and identify the pixels. Finally, the ANN was able to identify the pixels as cracks using "Numpy" commands, as shown in Fig. 7.

Artificial neural network

In the current study, neural network applications with various inputs were used to produce more accurate and user-friendly models by integrating basic computational tasks with parallel processes that simulate brain activity (compressive strength). Appropriate training and adaptation of neural networks will yield dependable outcomes. Artificial neural networks are information-processing models with predictive capabilities. Their purpose is to obtain knowledge from existing experimental, analytical, and theoretical data, as illustrated in Fig. 7. And it has been inspired by the neural network. The ANNs include inputs, hidden layers, and outputs, as shown in Fig. 7. The connections between elements are similar to synapses in neural networks, as shown in Fig. 7(b).

A layer of nodes, comprising an input layer, one or more hidden layers, and an output layer, makes up an artificial neural network (ANN). Every artificial neuron or node has a threshold and a weight that are related to one another. A node is activated and transmits data to the network's next layer if its output exceeds the designated threshold value. Otherwise, no information is sent to the subsequent network layer. The input, hidden layer, and outputs are all part of the artificial neural network's operation, as shown in Fig. 8.

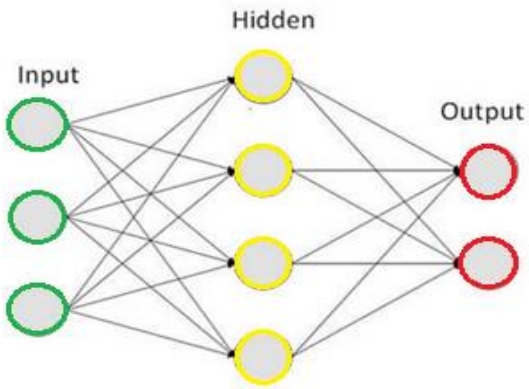


Fig. 8. Artificial neural network

This study established Python programming, and the ANNs were programmed using the Spyder plugin. The ANNs in the current study were coded using "NumPy," with more than 12 inputs, 144 hidden layers, and 5 outputs. Equation (7) was used to establish the

pixel parameters and displacements in this term, and as a result, it was able to forecast the location of each spot where a crack would occur:

$$y = ax + b. \quad (7)$$

Machine learning. The most popular technique in machine learning is regression analysis, which should be used to evaluate the predictive performance of machine learning (ML) algorithms using statistical indicators [45]. To create the model for forecasting the compressive strength of concrete, Ridge Regression (RR), Polynomial Regression (PR), and Linear Regression were typically taken into consideration. The Linear Regression (LR) algorithm's working formula is presented in Eq. (7).

According to Eq. (7), a and b represent the slope and the intercept coefficient, respectively. The polynomial function can take on different values with different coefficients (a_n). In addition, a_0 is the constant value or width from the origin of the polynomial function defined in Eq. (8):

$$y_{(x)} = ax_n x^n + a_{n-1}x^{n-1} + a_{n-2}x^{n-2} + \cdots + a_n x^n + a_0, \quad (8)$$

where x is a variable, $y_{(x)}$ is the dependent variable to x in Eq. (8), and a is the polynomial function's coefficient. The key statistical method used for calibration was Ridge Regression (RR), also known as the Tikhonov regularization [57]. This regression method employs a penalized estimator equation (9) to purposefully induce bias into the coefficient estimate, minimizing the variability of the estimations [26]:

$$\sum_{i=1}^{n}(y_i - X_i^T K - K_0)^2 + M\sum_{j=1}^{P} K_j^2, \quad (9)$$

where y_i represents the value of the dependent variable in the observation, X_i^T denotes the transposed value of X_i, K_0 represents the intercept coefficient, and K is the vector of regression coefficients.

The observation's vector of independent variables is represented by *i*, X_i; *i* represents the number of observations, n; the number of independent variables is represented by p; the order of the number of parameters is represented by *j*; and the *j*-th regression coefficient, within the total number of *p*, is represented by K_j.

Verification. Three techniques are used in this study to assess the accuracy and dependability of forecasting algorithms. The correlation coefficient (R^2) measures the model's ability to explain deviations in the desired characteristic (e.g., compressive strength) [52]. The average absolute deviation of anticipates from the experimental results is measured by the Mean Absolute Error, or MAE. The root mean square error (RMSE) for evaluating forecast errors significantly limits further deviations [20]. The correlation coefficient (R^2), as shown in Eq. (10), the mean absolute error (MAE), and the root mean square error (RMSE) were all evaluated to assess the forecast's validity. Considering Eq. (10), R^2 is a measure of the percentage of variation in the dependent component (such as concrete strength) that can be predicted based on the given characteristics (such as fiber content and curing time):

$$R^2 = 1 - \frac{\sum(y - \hat{}y)^2}{\sum^n (y - \bar{y})^2}, \quad (10)$$

where the actual, anticipated, and mean values are denoted by the letters y, $\bar{y}$ and $\acute{y}$, respectively. MAE calculates the average error between the anticipated and actual values, providing a clear assessment of model performance. According to Eq. (11), the MAE equation is equal to the sum of the numerical variations in the data sets divided by the integers. The MAE equation is defined by Eq. (11) as follows:

$$MAE = \frac{1}{n}\sum^{n}|y - \hat{y}|. \quad (11)$$

In addition, RMSE indicates larger prediction errors by calculating the root mean square of the errors. RMSE measures the average deviation between each actual data point and its corresponding predicted value:

$$RSME = \sqrt{\frac{1}{n}}\sum^{n}(y - \hat{y})^2. \quad (12)$$

Results and Discussion

Data analysis

The scatter plots shown in Fig. 9 represent the experimental and predicted compression strength test results, and the data analysis indicates that the experiment's outcomes and the forecast were pretty and similar.

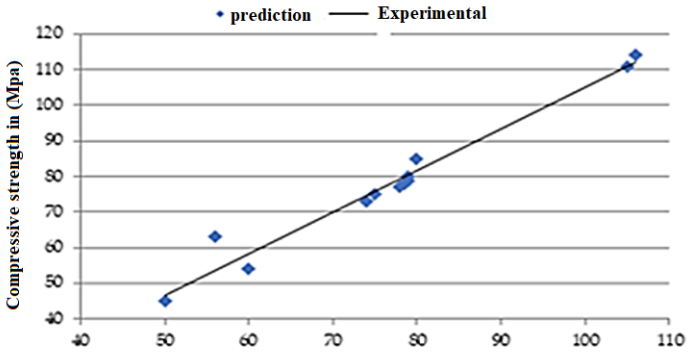


Fig. 9. Compressive strength prediction, and experimental results

Analysis of the machine learning algorithms' R^2, MAE, and RMSEs for each dataset reveals that the R^2 value was greater than 0.97, the MAE was greater than 2.1, and the RSME was higher than 16.99. The current study's Taylor diagram is shown in Fig. 10.

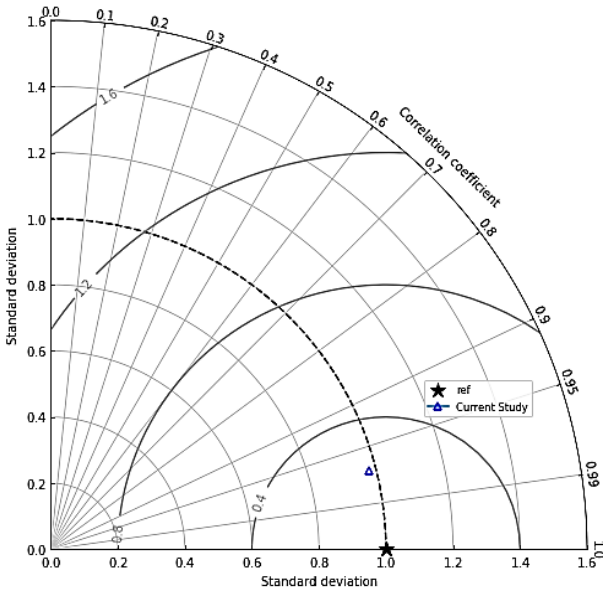


Fig. 10. Taylor diagram of the current study

Machine learning

The correlation matrix shows that basalt fiber has an adverse effect on the compressive strength of high-performance concrete. The impact of glass fibers was less than 17 %, and the effect of minibars was less than 81 %. Basalt fiber minibars had the most negative impact on concrete (Fig. 11).

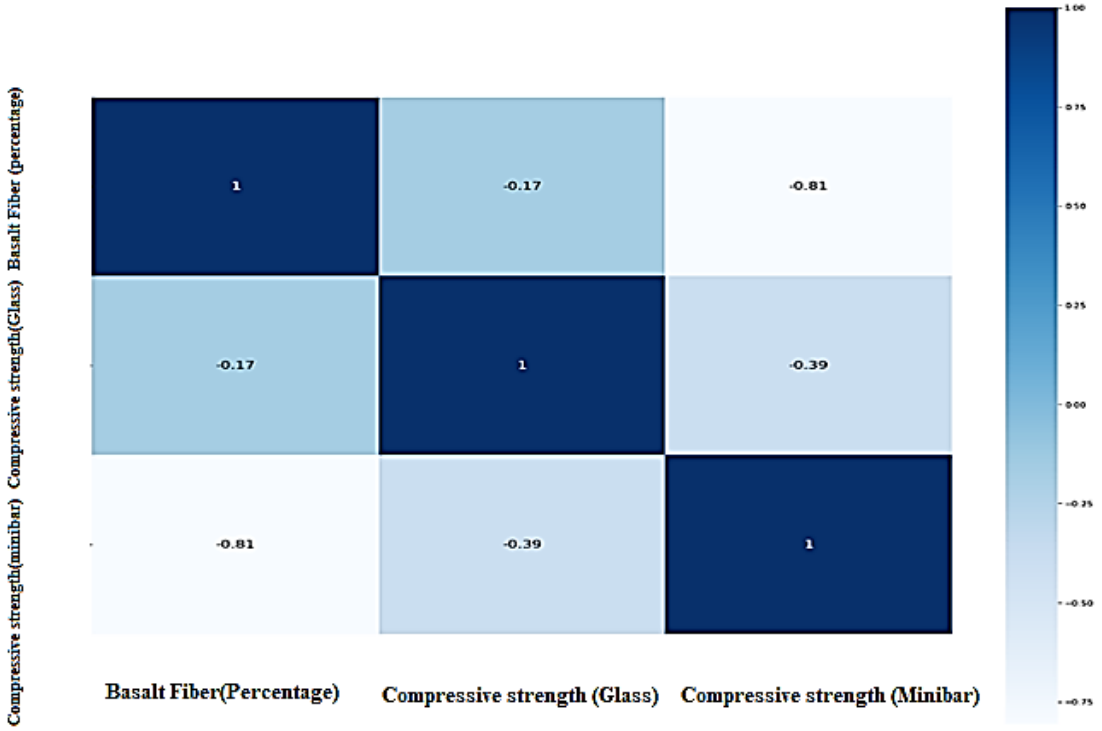


Fig. 11. Correlation matrix between compressive strength and basalt fiber

Figure 12 shows the LR and RR results of glass and minibars prediction. The results demonstrate that R^2 was 0.72 for both regression types. Therefore, LR and RR are not suitable methods for predicting compressive strength.

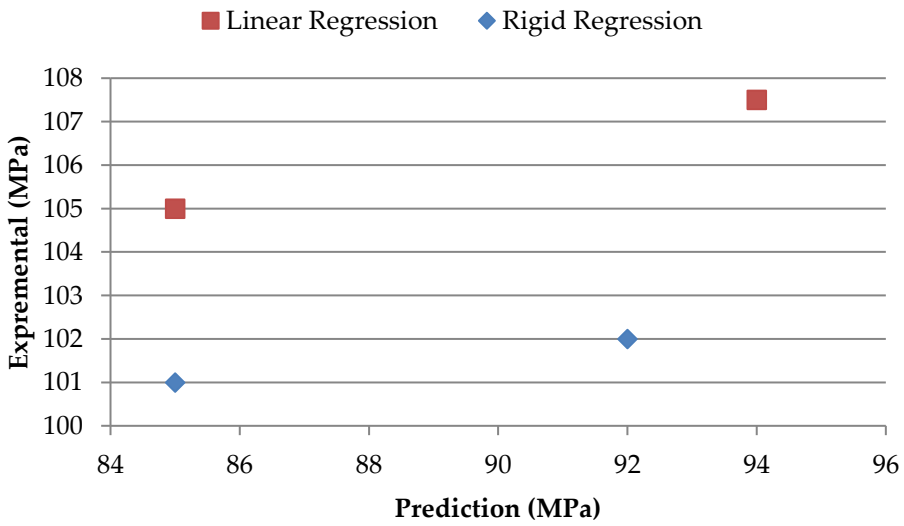


Fig. 12. Linear and Rigid regression results

Figure 13 displays the polynomial regression for glass fiber. The findings showed that the RSME was greater than 0.98, the MAE was greater than 0.21, and R^2 was greater than 0.93. Thus, as illustrated in Fig. 12, the PR results for glass fiber were appropriate and validated.

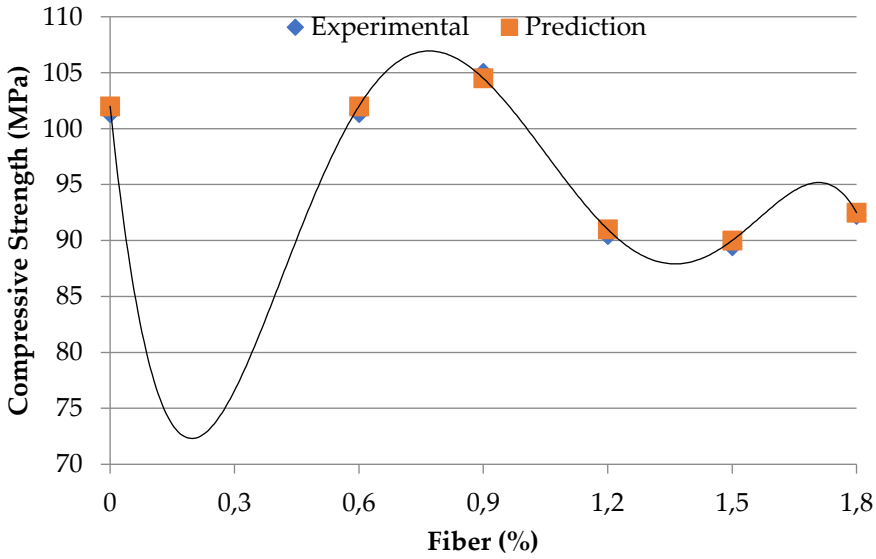


Fig. 13. Polynomial Regression g fiber

Figure 14 shows that the PR regression was based on minibar results. The findings indicate that the RSME exceeded 0.907, the MAE exceeded 0.25, and the R^2 exceeded 0.99. In general, the PR produced more inconsistent results than the LR and RR.

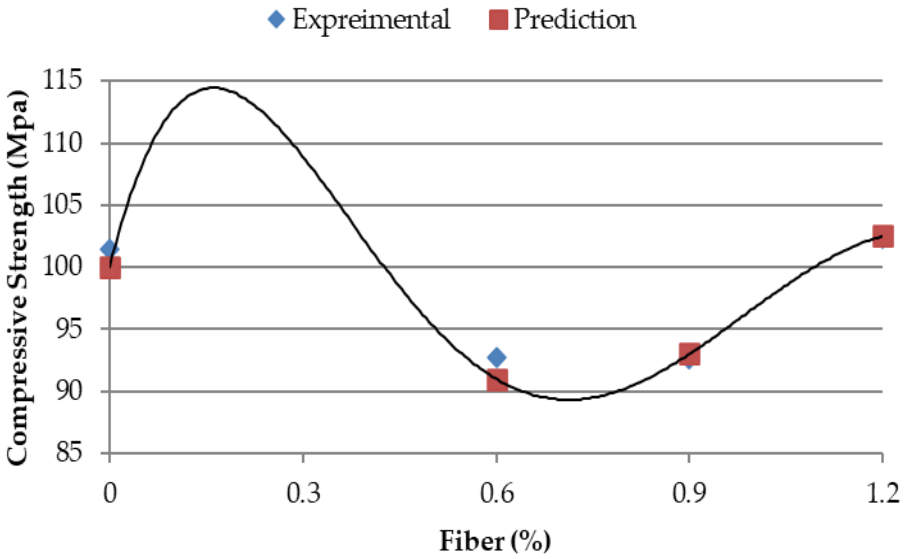


Fig. 14. Polynomial Regression Minibar basalt fiber

The Taylor diagram shows that the PR for minibars was closer to the references than for other regression types, as shown in Fig. 15.

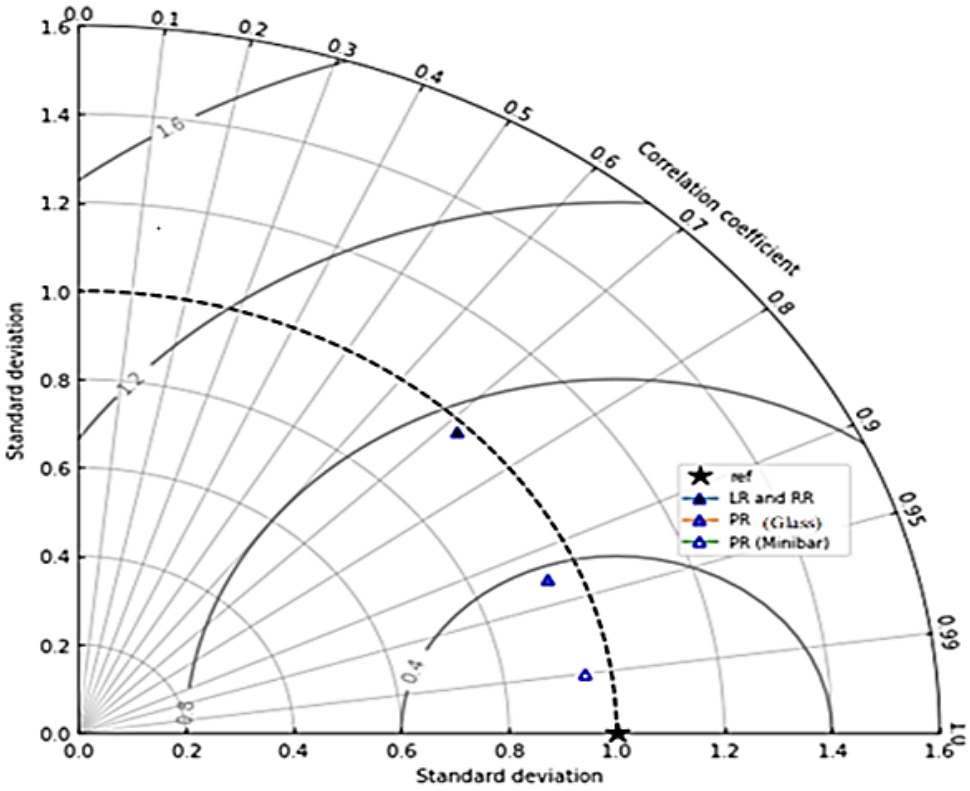


Fig. 15. Taylor diagram of the machine learning

Failure mechanism

Traditional cement-based concrete may eventually be replaced by concrete incorporating glass fiber and minibar basalt fibers. Figure 16 displays the ANN's experimental and pixel prediction results. By determining the cracking degree and maximum deformation length, the ANN was able to identify and forecast cracks on concrete surfaces, as shown in Fig. 16(a). The cube's cracking progress is displayed by the yellow pixels. The cube's pyramidal failure is shown in Fig. 16(b). ANNs that fail are shown in yellow in Fig. 16. By treating plot pixels as failure and crack locations, ANNs can accurately forecast the cube's failure mechanism using Eq. (6). A numerical assessment of the model's performance showed distinct error metrics and a high degree of compatibility. Specifically, the Root Mean Square Error was found to exceed 16.99, and the Mean Absolute Error exceeded 2.1, indicating the average magnitude of prediction errors. However, the coefficient of determination (R^2) was consistently greater than 0.97, indicating that the model explains over 97 % of the observed variance. The strong agreement between expected and real values was graphically evaluated using a Taylor diagram, which offered a clear statistical description of the fit between the predicted and experimentally measured compressive strength values. Among the numerous machine learning algorithms assessed, polynomial regression proved to be the most successful predictive model for this application. It demonstrated superiority by achieving high R^2 values for various composite materials, including over 0.93 for glass fiber-reinforced composites and over 0.99 for basalt fiber-reinforced composites. These findings highlight the model's outstanding accuracy, particularly in forecasting the compressive strength of basalt fiber composites.

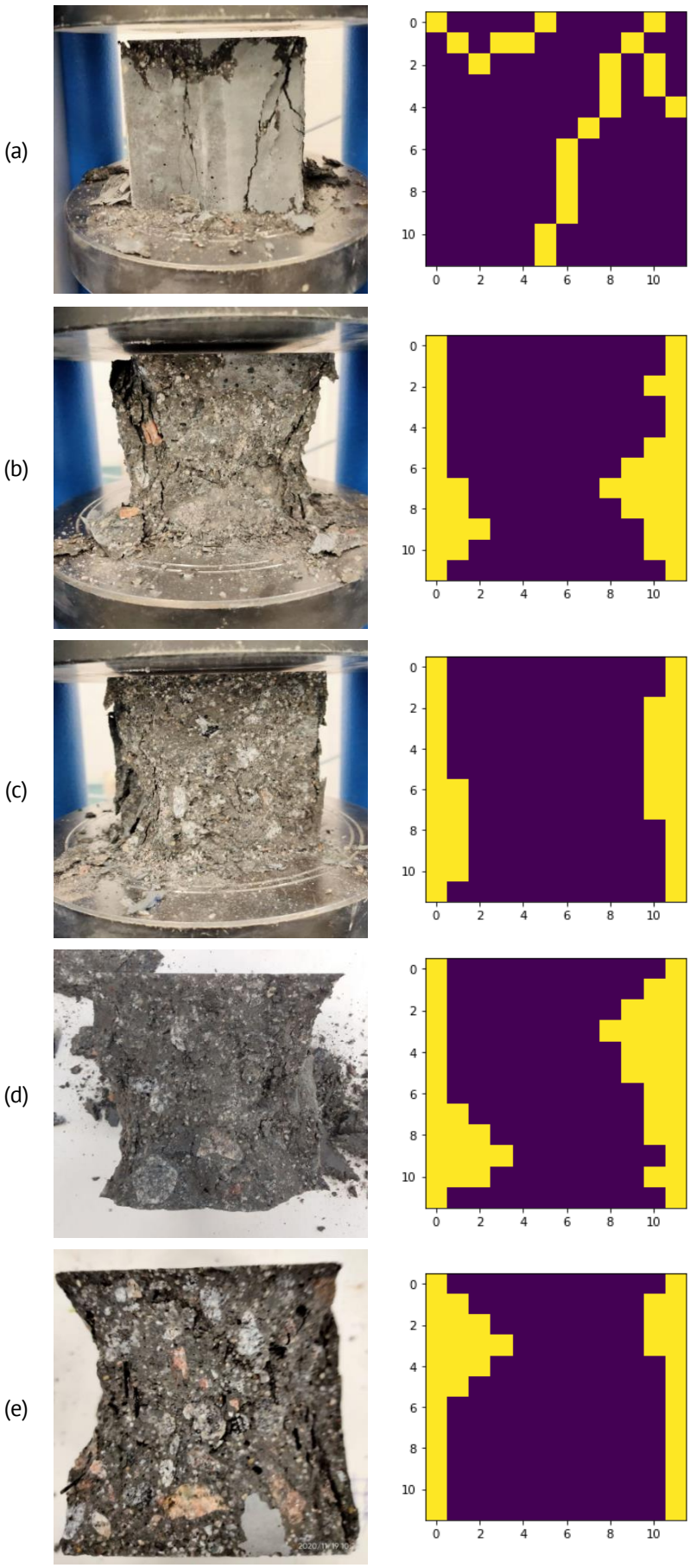


Fig. 16. Experimental results and pixel results in different stages

This investigation compares several constituents in High-Performance Concrete and evaluates compressive strength prediction using machine learning, artificial neural networks, and soft computing. While this study found that basalt fiber affects compressive strength, previous research has shown that it can improve HPC durability [53]. Machine learning predicts that polynomial regression produces good results for glass fiber and crystalline basalt fibers, with R^2 values of 0.93 and 0.99, respectively. Research was done to predict the characteristics of steel fiber-reinforced concrete beams under blast stress, and the results were compared [58]. The Gaussian Process (GP) regression they utilized has R^2 of greater than 0.9, which is higher than R^2 of 0.97 for PR. As an additional illustration, another researcher used machine learning to forecast structural behavior under explosion conditions [59]. They developed a program to model a reinforced concrete structure. Compared to the existing 99 % accuracy with PR for minibars and 93 % with glass fibers, they achieved 96 %.

Conclusions

This study analyzed compressive strength prediction by using soft computing, artificial neural networks, and machine learning techniques. The data from high-performance concrete with basalt fibers was imported into Python for a comparative examination of glass fiber and minibar basalt fibers. The results show that artificial neural networks (ANNs) are effective in forecasting both fracture patterns and the collapse of concrete cube surfaces under stress. This study indicates that engineers in construction can consistently predict the compressive strength of high-performance concrete using soft computing, machine learning, and, in particular, artificial neural networks. The essential research findings are described below:

1. The analysis demonstrated that the coefficient of determination (R^2) was over 0.97. The error measurements, Mean Absolute Error (MAE) and Root Mean Square Error (RMSE), were measured at values greater than 2.1 and 16.99, respectively. A Taylor plot clearly shows that the experimental and predicted compressive strengths are very similar.
2. Polynomial regression outperformed all other machine learning models tested in terms of accuracy. It produced high R^2 values, exceeding 0.93 for glass fiber-reinforced concrete and approaching 0.99 for combinations with crystalline basalt fibers.
3. The failure test results indicate a significant correlation and high similarity between laboratory-recorded results and model predictions.

CRediT authorship contribution statement

Nikolai I. Vatin: investigation, supervision, methodology, writing – review & editing, supervisor; **Mohammad Hematibahar:** data curation, experimentation, sample preparation, testing and characterization, writing – original draft; **Tesfaldet Gebre**: writing, sample analysis and review, formal analysis, Investigation.

Conflict of interest

The authors declare that they have no conflict of interest.

References

1. Ahmed T, Bediwy A, Azzam A, Elhadary R, El-Salakawy E, Bassuoni MT. Utilization of Novel Basalt Fiber Pellets from Micro- to Macro-Scale, and from Basic to Applied Fields: A Review on Recent Contributions. *Fibers*. 2024;12(2): 17.
2. Tahwia AM, Helal KA, Youssf O. Chopped Basalt Fiber-Reinforced High-Performance Concrete: An Experimental and Analytical Study. *Journal of Composites Science*. 2023;7(6): 250.
3. Lopresto V, Leone C, De Iorio I. Mechanical characterization of basalt fibre reinforced plastic. *Compos Part B*. 2011;42(4): 717–723.
4. Saleem A, Medina L, Skrifvars M. Mechanical performance of hybrid bast and basalt fibres reinforced polymer composites. *Journal of Polymer Research*. 2020;27: 61.
5. Arteiro A, Catalanotti G, Melro AR, Linde P, Camanho PP. Micro-mechanical analysis of the in-situ effect in polymer composite laminates. *Compos Struct*. 2014;116: 827–840.
6. Zhang P, Wang L, Wei H, Wang J. A Critical Review on Effect of Nanomaterials on Workability and Mechanical Properties of High-Performance Concrete. *Advances in Civil Engineering*. 2021;2021(1): 8827124.
7. Zuccarello B, Bongiorno F, Militello C. Basalt fibre hybridization effects on high performance sisal-reinforced biocomposites. *Polymers*. 2022;14(7): 1457.
8. Wei J, Mao X, Xu W, Xi C, Yan S, Sun T, Hu X, Wang Y, Chi F. Experimental Research on the Effect of Fiberglass on the Performance of Epoxy Asphalt Concrete. *Sustainability*. 2022;14(22): 14724.
9. Vu BT, Ngo TTH, Nguyen QD, Ngo AQ, Ho LS. Study on cement-treated soil with roadcem additive in construction of rural roads: A case study in Viet Nam. In: Ha-Minh C, Dao D, Benboudjema F, Derrible S, Huynh D, Tang A. (eds.) *CIGOS 2019, Innovation for Sustainable Infrastructure. Lecture Notes in Civil Engineering, vol 54*. Singapore: Springer; 2020. p.859–864.
10. Yakovlev GI, Grakhov VP, Drochytka R, Gordina AF, Nikitin SV, Begunova EV, Buriyanov AF, Repin AA. Modification of the structure and Properties of Fine-Grained Concrete with Carbon Black Dispersion. *IOP Conference Series: Materials Science and Engineering*. 2019;603(5): 052012.
11. Pandian A, Vairavan M, Jebbas Thangaiah WJ, Uthayakumar M. Effect of Moisture Absorption Behaviour on Mechanical Properties of Basalt Fibre Reinforced Polymer Matrix Composites. *J Compos*. 2014;4: 1–8.
12. Dharmendra Sondarva, Dr. Ankur C. Bhogayata. Usage of Chopped Basalt Fibers in Concrete Composites: A Review. *International Journal of Engineering Research*. 2017;6: 4085–4094.
13. Borhan TM. Properties of glass concrete reinforced with short basalt fibre. *Materials & Design*. 2012;42: 265–271.
14. Wei B, Cao H, Song S. Surface modification and characterization of basalt fibres with hybrid sizing. *Compos Part A Appl S*. 2011;42: 22–29.
15. Wei B, Cao H, Song S. Tensile behaviour contrast of basalt and glass fibres after chemical treatment. *Materials & Design*. 2010;31: 4244–4250.
16. Farooq F, Czarnecki S, Niewiadomski P, Aslam F, Alabduljabbar H, Ostrowski KA, Śliwa-Wieczorek K, Nowobilski T, Malazdrewicz S. A Comparative Study for the Prediction of the Compressive Strength of Self-Compacting Concrete Modified with Fly Ash. *Materials*. 2021;14(17):4934.
17. American Society for Testing and Materials. C109/C109M. *Standard Test Method for Compressive Strength of Hydraulic Cement Mortars (Using 2-in. or [50-mm] Cube Specimens)*. ASTM International; 2017.
18. Interstate Council for Standardization, Metrology and Certification. GOST 10180 – 2012. *Concretes. Methods for strength determination using reference specimens*. Moscow: Standardinform; 2018. (In Russian)
19. Ayub T, Shafiq N, Nuruddin MF. Mechanical properties of high-performance concrete reinforced with basalt fibers. *Procedia Engineering*. 2014;77: 131–139.
20. Vatin NI, Hematibahar M, Gebre TH. Chopped and minibars reinforced high-performance concrete: machine learning prediction of mechanical properties. *Frontiers in Built Environment*. 2025;11: 1558394.
21. Sun J, Wang J, Zhu Z, He R, Peng C, Zhang C, Huang J, Wang Y, Wang X. Mechanical Performance Prediction for Sustainable High-Strength Concrete Using Bio-Inspired Neural Network. *Buildings*. 2022;12(1): 65.
22. Amiri M, Hatami F. Prediction of mechanical and durability characteristics of concrete including slag and recycled aggregate concrete with artificial neural networks (ANNs). *Constr Build Mater*. 2022;325: 126839.
23. Stel'makh SA, Shcherban' EM, Beskopylny AN, Mailyan LR, Meskhi B, Razveeva I, Kozhakin A, Beskopylny N. Prediction of Mechanical Properties of Highly Functional Lightweight Fiber-Reinforced Concrete Based on Deep Neural Network and Ensemble Regression Trees Methods. *Materials*. 2022;15(19): 6740.

24. Yoon JY, Kim H, Lee YJ, Sim SH. Prediction Model for Mechanical Properties of Lightweight Aggregate Concrete Using Artificial Neural Network. *Materials.* 2019;12(7): 2678.
25. Feng W, Wang Y, Sun J, Tang Y, Wu D, Jiang Z, Wang J, Wang X. Prediction of thermo-mechanical properties of rubber-modified recycled aggregate concrete. *Constr. Build. Mater.* 2022;318: 125970.
26. Kumar A, Sen S, Sinha S, Kumar B, Nidhi C. Prediction of compressive strength of concrete doped with waste plastic using machine learning-based advanced regularized regression models. *Asian Journal of Civil Engineering.* 2025;26(4): 1723–1741.
27. Mashhadban H, Kutanaei SS, Sayarinejad MA. Prediction and modeling of mechanical properties in fiber reinforced self-compacting concrete using particle swarm optimization algorithm and artificial neural network. *Construction and Building Materials.* 2016;119: 277–287.
28. Erdik T. Discussion on "Prediction of compressive strength of concrete containing fly ash using artificial neural networks and fuzzy logic". *Computational Materials Science.* 2009;44: 1022.
29. Belalia Douma O, Boukhatem B, Ghrici M, Tagnit-Hamou A. Prediction of properties of self-compacting concrete containing fly ash using artificial neural network. *Neural Computing and Applications.* 2017;28: 707–718.
30. Mai HVT, Nguyen TA, Ly HB, Tran VQ. Prediction Compressive Strength of Concrete Containing GGBFS using Random Forest Model. *Advances in Civil Engineering.* 2021;2021(1): 671448.
31. Asri Y El, Aicha M Ben, Zaher M, Alaoui AH. Prediction of compressive strength of self-compacting concrete using four machine learning technics. *Materials Today: Proceedings.* 2022;57: 859–866.
32. Ali T, El Ouni MH, Qureshi MZ, Islam ABMS, Mahmood MS, Ahmed H, Ajwad A. A systematic literature review of AI-based prediction methods for self-compacting, geopolymer, and other eco-friendly concrete types: Advancing sustainable concrete. *Construction and Building Materials.* 2024;440: 137370.
33. Saridemir M. Genetic programming approach for prediction of compressive strength of concretes containing rice husk ash. *Construction and Building Materials.* 2010;24: 1911–1919.
34. Iqbal MF, Liu Q feng, Azim I, Zhu X, Yang J, Javed MF, Rauf M. Prediction of mechanical properties of green concrete incorporating waste foundry sand based on gene expression programming. *Journal of Hazardous Materials.* 2020;384: 121322.
35. Ngo TQL, Wang YR, Chiang DL. Applying Artificial Intelligence to Improve On-Site Non-Destructive Concrete Compressive Strength Tests. *Crystals.* 2021;11(10): 1157.
36. Candelaria MDE, Kee SH, Lee KS. Prediction of Compressive Strength of Partially Saturated Concrete Using Machine Learning Methods. *Materials.* 2022;15(5): 1662.
37. Fediuk R, Amran M, Klyuev S, Klyuev A. Increasing the performance of a fiber-reinforced concrete for protective facilities. *Fibers.* 2021;9(11): 64.
38. Chopra P, Sharma RK, Kumar M. Prediction of Compressive Strength of Concrete Using Artificial Neural Network and Genetic Programming. *Advances in Materials Science and Engineering.* 2016;2016(1): 7648467.
39. Khokhar SA, Ahmed T, Khushnood RA, Ali SM, Shahnawaz. A Predictive Mimicker of Fracture Behavior in Fiber Reinforced Concrete Using Machine Learning. *Materials.* 2021;14(24): 7669.
40. Khademi F, Behfarnia K, Behfarnia K. Evaluation of concrete compressive strength using artificial neural network and multiple linear regression models. *Iran University of Science & Technology.* 2016;6: 423–432.
41. Chen H, Sun Z, Zhong Z, Huang Y. Fatigue Factor Assessment and Life Prediction of Concrete Based on Bayesian Regularized BP Neural Network. *Materials.* 2022;15(13): 4491.
42. Tosee SVR, Faridmehr I, Bedon C, Sadowski Ł, Aalimahmoody N, Nikoo M, Nowobilski T. Metaheuristic Prediction of the Compressive Strength of Environmentally Friendly Concrete Modified with Eggshell Powder Using the Hybrid ANN-SFL Optimization Algorithm. *Materials.* 2021;14(20): 6172.
43. Kashyzadeh KR, Amiri N, Ghorbani S, Souri K. Prediction of Concrete Compressive Strength Using a Back-Propagation Neural Network Optimized by a Genetic Algorithm and Response Surface Analysis Considering the Appearance of Aggregates and Curing Conditions. *Buildings.* 2022;12(4): 438.
44. Kaplan G, Yaprak H, Memiş S, Alnkaa A. Artificial Neural Network Estimation of the Effect of Varying Curing Conditions and Cement Type on Hardened Concrete Properties. *Buildings.* 2019;9(1): 10.
45. Ahmad A, Ostrowski KA, Maślak M, Farooq F, Mehmood I, Nafees A. Comparative Study of Supervised Machine Learning Algorithms for Predicting the Compressive Strength of Concrete at High Temperature. *Materials.* 2021;14(15): 4222.
46. Dai L, Wu X, Zhou M, Ahmad W, Ali M, Sabri MMS, Salmi A, Ewais DYZ. Using Machine Learning Algorithms to Estimate the Compressive Property of High Strength Fiber Reinforced Concrete. *Materials.* 2022;15(13): 4450.

47. Nafees A, Javed MF, Khan S, Nazir K, Farooq F, Aslam F, Musarat MA, Vatin NI. Predictive Modeling of Mechanical Properties of Silica Fume-Based Green Concrete Using Artificial Intelligence Approaches: MLPNN, ANFIS, and GEP. *Materials.* 2021;14(24): 7531.
48. Song H, Ahmad A, Ostrowski KA, Dudek M. Analyzing the Compressive Strength of Ceramic Waste-Based Concrete Using Experiment and Artificial Neural Network (ANN) Approach. *Materials.* 2021;14(16): 4518.
49. Greco A, Maffezzoli A, Casciaro G, Caretto F. Mechanical properties of basalt fibres and their adhesion to polypropylene matrices. *Compos Part B Eng.* 2014;67: 233–238.
50. Bhat T, Fortomaris D, Kandare E, Mouritz AP. Properties of thermally recycled basalt fibres and basalt fibre composites. *Journal of Materials Science.* 2018;53: 1933–1944.
51. Sfarra S, Ibarra-Castanedo C, Santulli C, Paoletti A, Paoletti D, Sarasini F, Bendada A, Maldague X. Falling weight impacted glass and basalt fibre woven composites inspected using non-destructive techniques. *Composites Part B: Engineering.* 2013;45(1): 601–608.
52. Hasanzadeh A, Vatin NI, Hematibahar M, Kharun M, Shooshpasha I. Prediction of the Mechanical Properties of Basalt Fiber Reinforced High-Performance Concrete Using Machine Learning Techniques. *Materials.* 2022;15(20): 7165.
53. Vatin NI, Hematibahar M, Gebre TH. Impact of basalt fiber reinforced concrete in protected buildings: a review. *Frontiers in Built Environment.* 2024;10: 1407327.
54. Bai Y, Wierzbicki T, Bai Y, Wierzbicki T. Application of extended Mohr–Coulomb criterion to ductile fracture. *International Journal of Fracture.* 2009;161(1): 1–20.
55. Das P, Kashem A. Hybrid machine learning approach to prediction of the compressive and flexural strengths of UHPC and parametric analysis with shapely additive explanations. *Case Studies in Construction Materials.* 2024;20: e02723.
56. Hematibahar M, Esparham A, Vatin NI, Kharun MI, Gebre TH. Effect of gelatin powder, almond shell, and recycled aggregates on chemical and mechanical properties of conventional concrete. *Structural Mechanics of Engineering Constructions and Buildings.* 2023;19(2): 233–250.
57. Kamolov S. Comprehensive analysis of machine learning models for predicting concrete compressive strength. *Annals of Mathematics and Computer Science.* 2024;23: 119–130.
58. Almustafa MK, Nehdi ML. Machine learning prediction of structural response of steel fiber-reinforced concrete beams subjected to far-field blast loading. *Cement and Concrete Composites.* 2022;126: 104378.
59. Abd-Elhamed A, Alkhatib S, Abdelfattah AMH. Prediction of Blast-Induced Structural Response and Associated Damage Using Machine Learning. *Buildings.* 2022;12(12): 2093.